Proceedings World Geothermal Congress 2020+1
Reykjavik, Iceland, April - October 2021

Evolution of a Geothermal Brine from a Low-Temperature Radioactive Spring

DeBonne N. Wishart

International Center for Water Resources Management, Central State University, Wilberforce, OH 45384

dwishart@centralstate.edu

Keywords: geothermometry, thermal springs, geothermal resources, saturation indices, hydrogeochemistry.

ABSTRACT

Geochemical and fluid composition provide interesting insight on the diagenesis of a low-temperature geothermal brine and radioactive mineral spring (MKR) that emerges at base of the Carpenter's Mountain near the Milk River Mineral Hotel and Spa in Clarendon, Jamaica. A drastic shift of $\delta^{18}O$ and δD isotopes from the global meteoritic water line (GWML) indicates significant depletion of $\delta^{18}O$ and the enrichment δD in the region of influence from seawater. Concentrations of boron (B), lithium (Li), and strontium (Sr) reveal important information on the mixing of these geothermal fluids and seawater. Cationic ratios of Li/B vs. SO_4^{2-}/Cl^- indicate deep circulating fluid signatures derived mainly from ions leached during long water/rock interactions with weathered basement volcanic rocks and evaporites. MRT thermal waters containing dissolved $Radon^{222}$ are piped into the Milk River Mineral Hotel & Spa and diverted to Roman tiled baths for balneotherapeutic tourism. The heated geothermal brine ascends along fractures of the proposed active E-W trending, left-lateral strike-slip geostructure: the South Coast Fault (SCF). The SCF transects the Clarendon Plains and transfers motion to two of the island's restraining bends. Hydrogeochemical data suggests a more complicated underlying structure at the site. A hypothetical model of the hydrodynamic saline fluids migrating from the geothermal system along permeable fractures of the South Coast Fault is conceptualized from hydrogeochemical, isotopic, geological, and structural data. Brines are classified based on their high Cl^- concentration and are classified as a concentration of >10000 mg/L total dissolved solids (Davis, 1964).

1. INTRODUCTION

1.1 Water Rock Interaction

The extent of water-rock interaction, residence time, and the geological setting influence the chemical composition and temperature and chemistry of the waters discharging from mineral springs. Cold spring waters in the absence of borehole data or wells may provide pertinent information about the subsurface geology and hydrological processes such as shallow mixing between circulating geothermal fluids, meteoritic recharge or no mixing at all. Pattern recognition of ions in fluids has been used to quantitatively trace the evolution of thermal waters (Cruz and Franca, 2006; Delgado-Outeiriño et al., 2009; Pasvanğolu, 2013) and groundwater composition (Knauth 1988; Fontes and Matray, 1993; Dassi, 2011). Environmental and radioactive stable isotopes are used to qualitatively and quantitatively identify the origin; mixing between meteoritic and geothermal waters; and mixing between surface and groundwater. The chemical composition of geothermal fluids may be enriched by a variety of inorganic ions including Cl^-, Na^+, and Ca^{2+} enriched due to halite (NaCl) and calcite ($CaCO_3$) dissolution; and dissolved gases. Geothermal fluids are classified based on salinity and delineated based on interaction with deposits in sedimentary basins or surrounding crystalline rocks (Drever et al., 2004). Salinity concentrations in thermal and cold waters are based the on availability of soluble salts (e.g. evaporites) in sedimentary basins (Kharaka and Hanor, 2004) and possible prolonged water-rock interaction with connate water. Evaporite dissolution is one of two major water-rock interactions proposed as a mechanism allowing meteoritic water to evolve into concentrated brines in sedimentary basins (Knauth, 1988). Ionic ratios of SO_4/Cl vs. Li/B are used to indicate deep circulating fluid signatures derived mainly from ions leached during long water/rock interactions with very saline environments and weathered basement volcanic rocks (Leeman and Sisson, 1996). Processes such as evaporation, recharge under different conditions, dilution, mixing from different sources influence the stable isotope (δ^2H and $\delta^{18}O$) compositions of waters. Oxygen-18 ($\delta^{18}O$) and deuterium (δ^2H) isotope analyses of thermal and cold water springs are used to assess the origin of geothermal fluids, source, water-rock interaction processes, and mixing between fluids. Geothermal fluids mixed with other water also increases the $\delta^{18}O$ content of waters and decreases the $\delta^{18}O$ content of rocks as water and rock attempt to reach a new state of isotopic equilibrium at an elevated temperature. This results in a shift in an oxygen shift of the $\delta^{18}O$ values, but not the δ^2H values of geothermal waters. The increase in geothermal gradients with increasing temperature and depth not only raises the temperature of fluids that discharge at the surface, but allows extensive mixing between fluids. Non-volcanogenic thermal springs may be associated with regional tectonism (including active faulting) rather than magmatism.

1.1.1 Alkali Metals as Tracers of Geothermal Fluids

The alkali metals Cl, B, and Li are conservative of which Li is least affected by secondary processes. Li, B, and Cl are not equilibrated in the fluid phase; therefore they may be used as geoindicators of the deep rock dissolution process and origin of circulating geothermal fluids (Brondi, 1973; Brondi, 1983; Delgado-Outeiriño et al., 2012). Boron is highly soluble; is salinity-dependent (Lee et al., 2010); long residence time in seawater (Lemarchand et al., 2002; and tends to concentrate in environments of limited circulation, evaporites, or bines of marine or terrestrial origin (Uhlman, 1991). The rate at which fluids travel to the surface may be indicated by the concentration of Li^+; for example, higher Li^+ concentrations tend to be associated with fluids travelling rapidly to the surface as the short water-reaction time does not involve its incorporation with clays and zeolites (Delgado-Outeiriño et al., 2000). Chloride (Cl^-), boron (B^+) and lithium (Li^+) are geochemically mobile and are the best tracers of evaporitic solution and successive mixing in the formation of brines and the entire interval of seawater formation (Fontes and Matray, 1993). SO_4/Cl vs. Li/B ratios may be used to delineate water samples from aquifers with long residence times and indicate the depth of circulation and mixing of geothermal fluids. (Sánchez-Martos et al. 2004).

1.2 Solute and Chemical Geothermometry

The chemical signature of a solute concentration (i.e. solute ratios) is assumed to indicate the hot equilibrium temperature stored in the ascending fluid. Therefore, discharge temperatures of spring water have been used in many hydrogeochemical investigations to estimate geothermal reservoir temperatures from chemical geothermometers (Mohammadi et al., 2010; Shakeri et al., 2008; López-Chicano et al., 2001). The temperature dependency on the concentration ratios of the liberated cations (Ca^{2+}; Na^{+}; Mg^{2+}; K^{+}) makes it possible to calculate the water temperature as water-rock interaction is slow, possibly up to thousands of years. Cation and silica solubility type geothermometers are based on temperature-dependent, mineral-solution equilibria attained between circulating waters and host rocks of the geothermal reservoir. The application of chemical geothermometers is based on the assumption that during their ascent fluids may release CO_2) from contact with the geothermal source; re-equilibrate or undergo dilution with shallow circulating fluids, undergo conductive heat loss proportional to the distance travelled and inversely proportional to the flow rate resulting in an underestimation of geothermal reservoir temperature. However, the temperature of a geothermal fluid sampled at the surface may not be a temperature indicator of the subsurface reservoir. Geothermometric equations and ternary graphs are mixing models that are used to estimate the minimum subsurface temperature from the analyses of thermal waters or hot springs present in the regional area of interest (ROI) of a given area. Estimated geotemperatures are deemed more dependable if the results from several techniques are in agreement. A more reasonable estimate of the geothermal reservoir temperature may be determined by comparing reservoir temperatures estimated from geothermometric equations with temperature estimated from other models e.g. the Giggenbach (1988) trilinear geotemperature indicator and the SolGeo computer program (Verma et al., 2008), etc. to derive a more reliable estimates of the reservoir temperature.

The integration of mineral spring hydrogeochemistry integrated with information on tectonic setting of a ROI are invaluable to tracing fluid evolution and the conceptualization of active chemical processes (e.g. mixing between meteoritic recharge and geothermal fluids) and the influence of structure on hydrological process leading to the discharge of Milk River thermal spring and Salt River cold mineral spring along the western and eastern periphery of the Clarendon Basin, in south central Jamaica. The objective of this investigation is to (1) apply several pattern recognition and analytical techniques, (2) estimate the geotemperatures at the depth of MKR circulation, and (3) conceptualize the evolution of the MKR and SRS waters migrating from permeable fractures in close proximity to the South Coast Fault based on hydrogeochemical data and information on geological and tectonic setting. In this paper, pattern recognition; ion ratios; and stable isotopes are used to trace the evolution of both the MKR and SRS waters. Geothermometric modeling is used to estimate the geotemperatures at the MKR a geothermal source.

2. GEOLOGICAL SETTING AND STRUCTURE OF THE STUDY AREA

2.1 Location of Study Site

Milk River thermal spring (MKR) discharges at 1.2 m above sea level (ASL) from a north-northeast-striking fault (Vincenz, 1959) by the base of Round Hill, just south of the South Coast Fault Zone (SCFZ) in Clarendon Parish, Jamaica (Figure 1). Round Hill is bordered by Carpenters Mountain, a NNE-striking anticline, (Figure 1). The spring emerges at the geological contact between the Miocene age Newport Formation of the White Limestone Group and the overlying Quaternary Alluvium sediments that blanket the Clarendon Plains. Salt River spring (SRS) is located 2.7 km east of MKR and also in close proximity to the South Coast Fault (SCF). SRS emerges from fractures in the White Limestone near the Brazilletto Mountains and discharges to a very large pond hydraulically-connected to Salt River Bay. MKR and SRS are two of three radioactive springs on the island, the third is Windsor spring (WS) located on the banks of St. Ann's Great River in north central Jamaica (Hylton, 1987).

Clarendon Plains is a Late Miocene age sedimentary basin situated north of the SCFZ in south central Clarendon (Figure 1).. Its aerial extent is 80 mi^2 (207 km^2) at elevations of 0-150 m above sea level. The White Limestone is Jamaica's principal aquifer and it is incised by a well-developed interconnected network of fractures in the upland regions bordering Clarendon Plains and to the southeast at Portland Ridge. The Newport Formation consists of moderately well-bedded, compact limestones with some rubbly layers. The Quaternary Alluvium is bordered by Carpenters Mountain to the west; Mocho Mountains to the north; Brazilletto Mountains to the east; and lies in Vere Plains to the south (Taylor and Chubb, 1956). The Alluvium forms the island's second aquifer reaching thicknesses of 100 m north of the SCF and a maximum of 650 m south of it (Wadge et al., 1985). Borehole data indicate the lithology of the Quaternary-Age alluvium consists of fluvial deposits of volcanic and volcanogenic clasts derived from the Cretaceous volcanic basement (Howard and Mullings, 1996). A basal clay unit separates the alluvium from underlying Newport Formation, except in areas where the alluvium crops out against it and fills fault-incised channels.). The Rio Minho River and Milk River (no relation to the spring at MKR) flow southwards over Clarendon Plains. The alluvial fan of the Rio Minho extends south beyond the South Coast Fault (SCF) to Vere Plains where the water table rarely exceeds 20-25 m (Howard and Mullings, 1996). Vere Plains south of the SCFZ is blanketed by an area of alluvium 37 mi^2 (96 km^2.

2.2 Tectonic Setting

The Caribbean island of Jamaica (Figure 2) is located on the extended tip of the Nicaraguan Rise, a Cretaceous submarine volcanic plateau extending 700 km NE-SW from Nicaragua, Central America to the island (Lewis and Draper, 1990; Robinson, 1994; Arden, 1995). Jamaica underwent a period of arc volcanism during which andesitic and basaltic lavas (Meschede and Frisch, 1998) were extruded to form volcanic basement rock (Roobol, 1976). Jamaica lies within a geologically-young and seismically-active fault zone that evolved in a restraining bend (Figure 2 and 3) on the E-trending, left-lateral boundary between the Gônave Microplate and Caribbean Plate during the Miocene Epoch over 23 million years ago (Mann et al. 2007; Benford, et al. 2012; Domínguez-González et al., 2015). The island underwent subsidence by a marine transgression and the subsequent growth of an extensive carbonate platform during the Early Cenozoic Era, approximately 45 million years ago (MYA). Tertiary carbonates (Benford et al., 2012b) including initial deposits of limestone intercalated with terrigenous volcanogenic debris from eroded remnant volcanoes were deposited to form the Cretaceous Yellow Limestone Group. The impure Yellow Limestone was succeeded by the deposition of the White Limestone Group (that covers approximately 70% of the island) approximately 30 MYA. Phases of sedimentary deposition were accompanied by changes in tectonic stress regimes and or tectonic events (Draper, 1998). Benford et al. 2015 suggests E-striking faults like the Cretaceous age SCF are currently reactivated as transfer zones within the contractual restraining bend and the presence

of E-W striking and NNW striking fault sets are evidence of neotectonic deformation in Jamaica. Fault zones may act as effective conductive conduits for fluid flow and also as barriers to fluid flowing across faults, if sealed (Caine et al., 1996).

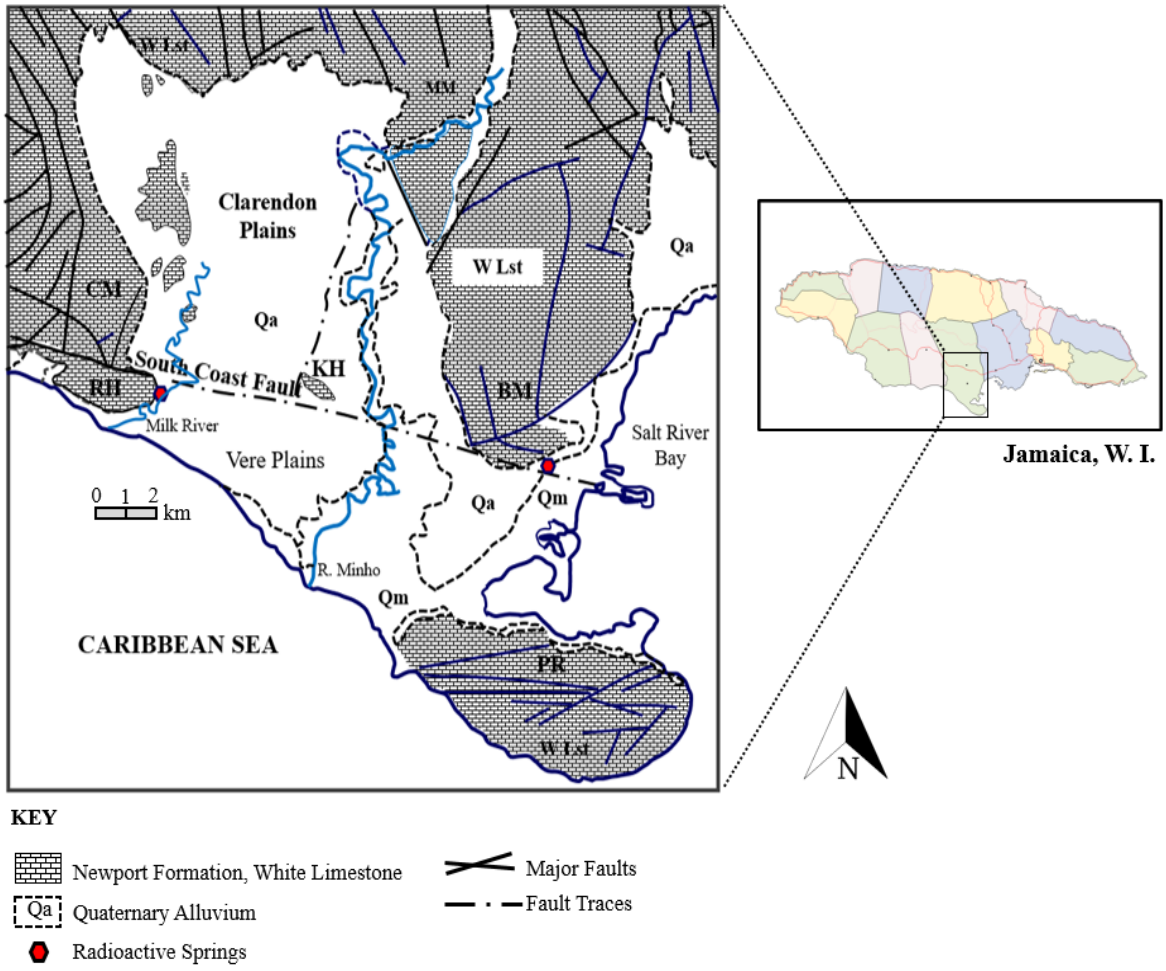

Figure 1: Simplified geology of the location of the Milk River thermal spring (MKR) and Salt River cold water spring (SRS) field sites with the surrounding Clarendon and Vere Plains basins. Structural features include RH-Round Hill; CM-Carpenters Mountain; MM-Mocho Mountains; BM-Brazilletto Mountains; PR-Portland Ridge; and the east-west striking SCF- South Coast Fault.

2.2.1 The South Coast Fault Zone (SCFZ)

The South Coast Fault (SCF) is a major east-west striking (Fig. 1 and Fig. 3), strike-slip fault (Benford et al. 2015) that borders the Clarendon Plains sedimentary basin. It is proposed the SCFZ acts as a left-lateral, strike-slip 'bypass' fault that truncates a large, right-stepping restraining bend formed between the Plantain Garden fault zone of southeastern Jamaica and the Duanvale-Walton fault zone of northwestern Jamaica (Benford et al. 2015). Mann et al. 2007 interpreted the SCF as a fault set against which deformed NNW-trending ranges and faults of southern Jamaica terminate, transfers motion to two of the island's restraining bends that accommodate contraction and crustal shortening, and forms a scarp as high as 600 m in areas along the southern coast of Jamaica (Benford et al. 2015). Figure 3 illustrates the SCFZ truncates a major, right-stepping restraining bend formed between the Plantain Garden Fault Zone (PGFZ) in southeastern Jamaica and the Walton Fault Zone (WFG) of northwestern Jamaica. Benford et al. 2015 interpreted rock density contrast along a graben aligned with the SCF (and also forms Vere Plains) from their two-dimensional gravity and geodetic modeling study. The graben delineated by their study could possibly act as a permeable pathway for the flow of fluids to sediments extending across Clarendon Plains and Vere pains and via fractures that act as conduits for flow. It is possible, the tectonic setting of the SCF that transects Clarendon Plains and Vere Plains responsible for the non-volcanic geothermal conditions in the area amendable to geothermal exploratory drilling.

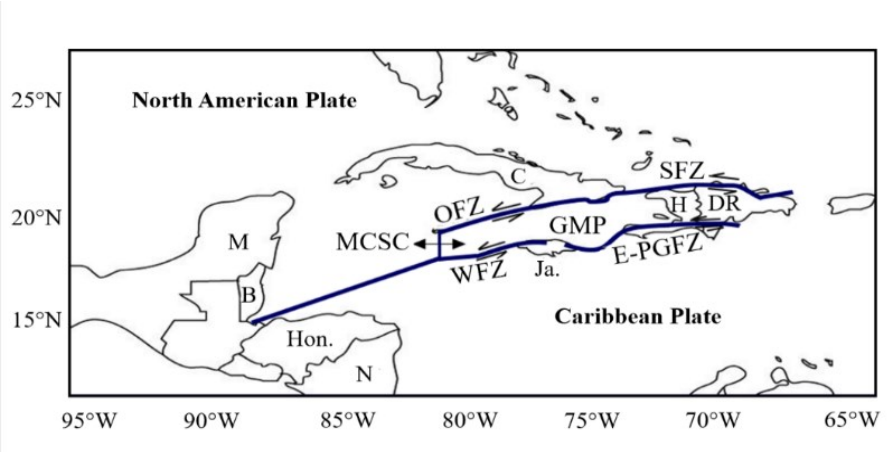

Figure 2: Location of Jamaica in a restraining bend on the E-striking, left-lateral plate boundary between the Gônave Microplate and Caribbean Plate during the Miocene epoch over 23 million ago (Benford et al., 2012b). [GMP- Gonaive Microplate; ORFZ -Oriente Fault Zone; SFZ- Septentrional Fault Zone; WFZ - Walton Fault Zone; E-PGFZ - Enriquillo-Plantain Garden Fault Zone; MCSC-Mid Cayman Spreading Center; Ja-Jamaica; H-Haiti; Hon.- Honduras; DR - Dominican Republic; M-Mexico; B-Belize; N-Nicaragua.]

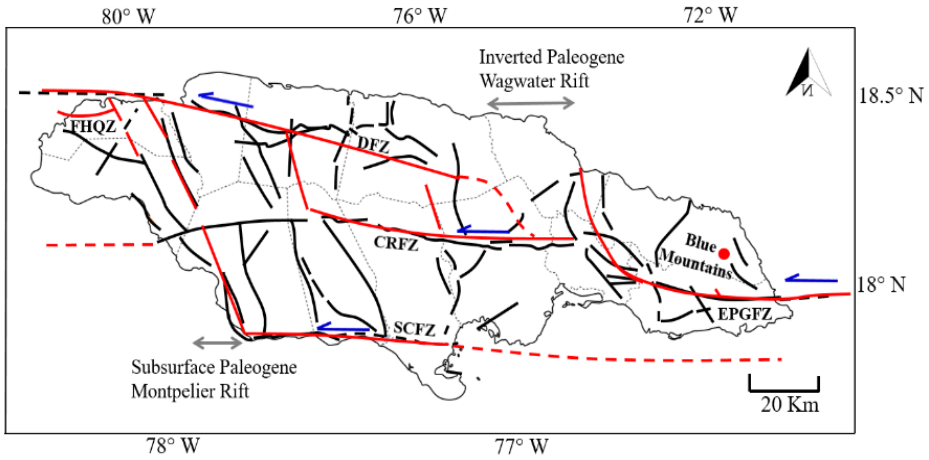

Figure 3: Tectonic map of Jamaica. EPDFZ = Fault Zone; SCFZ = South Coast Fault Zone; CRFZ = Crawle River Fault Zone; FHQZ = Zone, and the DFZ = Duanvale Fault Zone. [This diagram was modified after Mann et al., 2007 and Benford et al., 2015].

2.3 Balneology and Radioactivity

Milk River thermal spring (MKR) (Figure 1) is notably one of the most radioactive springs in the world. The radioactivity level of water is classified as light radioactive water (< 5 Bq/L); intermediate radioactive water (between 1,100 and 5,550 Bq/L), or strong radioactive water (> 5,550 Bq/L). Radioactivity in MKR water is entirely from Rn^{222} = 16020 µCi/L = 5.92 X 10^8 Bq/L (Barnett, 1923; Vincenz, 1959; Hylton, 1987). It is important to mention here that not all radioactive springs are thermal. MKR water is world renowned for its therapeutic MKR water advertised as being 54 times more radioactive than the waters of Baden (Switzerland); 50 times more radioactive than the waters of Vichy (France); 9 times more radioactive than the waters of Bath (Somerset, England); and 3 times more radioactive than the waters of Karlovy Vary (Czech Republic). The flow rate of the spring is 20-60 L/sec and some water is piped 20 meters east where its outflow to a well is 0.03 L/sec. The water is diverted to the Roman tiled baths at the Milk River Hotel & Spa for balneotherapeutic tourism. Milk River Spa patrons bathe in the water for a maximum of 20 minutes, not exceeding three times/day for treatment of the central and peripheral nervous system; osteoarthritis; and other disorders of the bones, joints and muscles [i.e. rheumatism, neuralgia, sciatica, lumbago, gout] (Zans, 1961). Tourists and local residents east of MKR, bathe in a large pond hydraulically-connected to Salt River Bay and filled by discharges from cold mineral water from Salt River spring (SRS).

3. METHODOLOGY

Spring water samples were collected from MKR and SRS sites and processed at analytical laboratories for ion and isotopes concentrations. The data quality assurance included the introduction of internal reference samples and analyses of three sets of duplicates for water samples from each of the sites. Data precision was found to be within International standards. AquaChem® and RockWare AqQA® software were used to classify water type, perform ion balance; and model mineral phase equilibria for the MKR and SRS datasets. Ionic ratios, graphical representation, and ternary diagrams were used to improve the classification, geochemical signature, and understanding of the geochemical processes leading to the evolution of the MKR and SRS waters.

4. RESULTS AND DISCUSSION

4.1 Hydrogeochemistry

Table 1 lists the physiochemical parameters and concentrations of major and minor ions in the MKR thermal and SRS cold water samples. Temperature, pH, and ion concentrations (i.e. Na, Mg, K, Cl, B, and Sr) are generally higher in the MKR sample. Figure 4a is a Schoeller (1962) semi-logarithmic plot that represents major ion analyses in milliequivalents per liter and classifies MKR and SRS as Na-Cl hydrochemical water types based on their relative concentrations of major cations and anions. An alternative to the Piper (1944) ternary diagram is the Durov diagram (Durov, 1948) that demonstrates the relationship between various ions as percentages of milliequivalents in MKR and SRS samples (Figure 4b). Na-Cl waters are typical of marine and deep ancient ground waters. The variation in the Na-Cl mass ratios for MKR and SRS may be attributable to the depth of circulation and permeability of the fracture network associated with the South Coast Fault Zone (SCFZ).

Table 1: Physiochemical paramters and concentrations of major and minor ions in the MKR and SRS water samples

ID	T (°C)	pH	TDS (ppm)	EC (µS/cm)	ORP (mV)	DO (%)	Na^+ (mg/L)	Ca^{2+} (mg/L)	Mg^{2+} (mg/L)	K^+ (mg/L)	B^+ (mg/L)
MKR	36.6	7.13	35000	54600	79	130	12000	860	1100	850	7.10
SRS	29.7	8.04	12943	24242	164	378	2800	340	350	250	2.30
ID	**Li^+ (mg/L)**	**Sr^{2+} (mg/L)**	**Rb^+ (mg/L)**	**Cl^- (mg/L)**	**Br^- (mg/L)**	**F^- (mg/L)**	**SO_4^{2-} (mg/L)**	**HCO_3^- (mg/L)**	**HS^- (mg/L)**	**SiO_2 (mg/L)**	
MKR	0.55	8.1	0.070	17600	40.8	1.3	291	113	0.029	9.4	
SRS	0.17	3.7	0.250	7700	16.8	0.7	344	238	0.029	12.1	

The Chebotarev (1955) paper on patterns in groundwater chemistry, describes increased salinity in groundwater accompanied by change in the dominant cation from Ca^{2+} to Na^+ with increasing residence time and age. Cation exchange as a hydrochemical process leads to either alterations or reversals in the cation sequences such as prior mentioned; therefore, caution is exercised when referring to the general cation sequences depicted by Chebotarev (1955). Waters with shorter residence times are dominated by Ca^{2+} [i.e. (Ca^{2+}>Mg^{2+}>Na^+)], whereas Na^+ dominate in waters with longer residence time [i.e. (Na^+> Mg^{2+}>Ca^{2+})]. MKR and SRS waters are dominated by the ion sequence Na^+> Mg^{2+}>Ca^{2+} implying longer residence time and deep fluid-fluid equilibria (Table 1). The diagenetic effects of ion exchange may account for higher Ca^{2+} concentrations in the MKR and SRS waters. Higher Mg^{2+} concentrations in MKR compared SRS waters may be due to the exchange of Mg^{2+} for Ca^{2+} at low temperatures (Collins, 1975). In particular, the 35,000 ppm TDS concentration of in MKR appeared to reduce to 15540 ppm during fluid migration along fractures en route to SRS. The waters discharges at a lower temperature of 29.7°C. The high TDS values and boron concentrations for MKR and SRS waters are related to major ion chemistry Cl^-, Na^+, and Ca^{2+} concentrations indicative of long water-rock interaction and evaporite dissolution from a common geothermal source. The total dissolved solids (TDS) concentration is an indication of the extent of water-rock interaction deep in the subsurface and possibly as the ascent of the waters. Although not graphed here, the presence of strontium (Sr^{2+}) appears to be related to water-rock interaction with the volcanic basement and fluid-fluid mixing in the MKR and SRS samples.

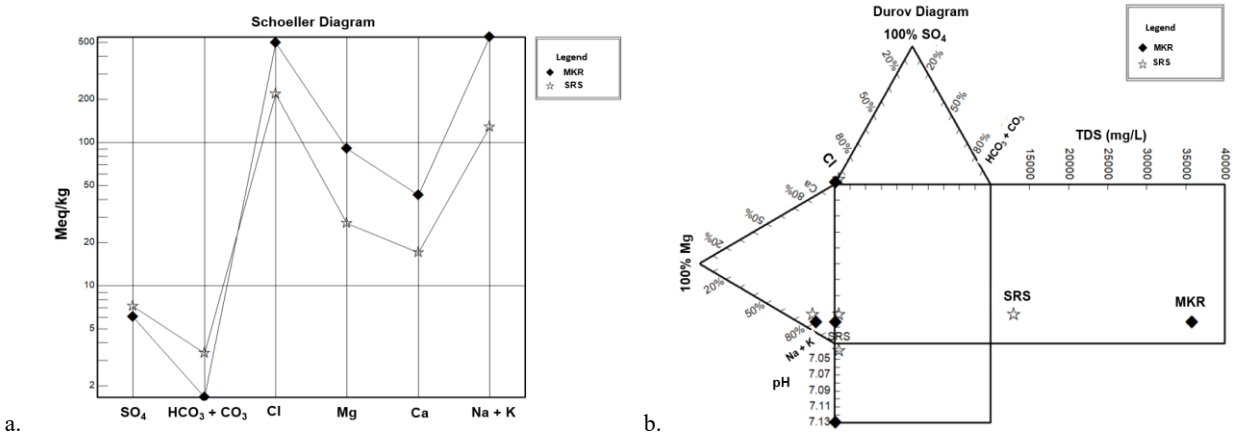

a. b.

Figure 4: a. Schoeller (semi-logarithmic) diagram representation of major ion analyses (meq/l) and hydrochemical water type for MKR and SRS, b. Durov diagram showing major ions and TDS concentrations with pH for MKR and SRS samples.

4.1.1 Ionic Indices and Ionic Ratio Analyses

Ion concentrations and ionic ratios investigated during exploratory data analysis revealed interesting results regarding the evolution, mixing, depth of circulation, and hydrological processes influencing the MKR and SRS water samples. Cl^- appears to be the dominant ion that has travelled in deep groundwater for long distances along flow paths. Further insights into the conservative behavior of chloride with other ions as indicators of the extent of water-rock interaction, depth of fluid circulation, and origin were highlighted from graphical analyses of (1) Log Cl^- vs. B^+; (2) Cl^- vs. Br; (3) SO_4^{2-}/Cl^- vs. Li^+/B^+; and (4) Cl-Li-B ternary diagram by Giggenbach (1991) plotted for the MKR and SRS water samples. Figure 5a shows increases in Cl^- are exponentially correlated with increasing B^+ concentration in the waters from all three radioactive springs of Jamaica: MKR, SRS, and Windsor spring (WS). Sample (WS) is a Ca-Na-C-type water with concentrations of TDS (23940 Mg/L), B (19 mg/L), T = 29.7°C, and radioactivity (Rn^{222} = 0.23µCi/L = 8.51 X 10^3 Bq).

Increases in Cl^- are linearly correlated with increasing Br^- in Figure 4b. The highest B and Li values are observed in waters with long residence times and extensive interaction rock-water interaction; therefore, Li/B ratios may be related to the depth of an aquifer

(Delgado-Outeiriño et al., 2000). Cl and SO_4 enrichment in groundwater is may result from mixing with seawater or the dissolution of evaporites. The graph of SO_4^{2-}/Cl^- vs. Li^+/B^+ for MKR and SRS in Figure 5c show the influence of the Cl^- ion in a deeper aquifer, longer residence times and mixing with sweater, and the formation of Na-Cl brines from a common source compared to a shorter residence time for a hot spring sample from the Bath (BTHN and BTHS) in eastern, Jamaica. MKR and SRS are the result of the mixing between primary and secondary brines from one common origin (Hylton, 1987). The Cl-Li-B ternary diagram (after Giggenbach et al., 1991) in Figure 5d illustrates the relative concentrations of Cl, B^+, and Li^+ in MKR and SRS waters. Both MKR and SRS plot directly in the 'seawater' field characterized by high Cl, neutral-pH, and mature waters and from an old hydrothermal system. The 'old hydrothermal system' may have involved heating of remnant seawater trapped in older limestone rocks of the carbonate platform above an ancient volcanogenic basement associated with the collision of the oceanic plateau with an island arc (Section 2.2). Upward flowing waters of geothermal systems tend to have chloride-rich waters. Relative to seawater, geothermal fluids are enriched in Cl^+, but depleted in cesium (Cs). Cesium was not detected in either the MKR or SRS water sample. Chloride concentration plays a dominant role in the evolution and mixing of MKR and SRS water samples from the source to the point of discharge and may be inferred from the fit of the data to the type of equation in each of the cases of Figure 5a – 5c. For example, the curve of SO_4^{2-}/Cl^- vs. Li^+/B^+ ratio, the data fits a polynomial equation (Figure 5c). Na-Cl waters are typical of marine and deep ancient ground waters and the variation in the Na-Cl mass ratios for MKR and SRS may be attributable to the depth of circulation controlled by the fracture network in the SCFZ. The regional tectonic setting of the SCF and its close proximity to the MKR and SRS sites, including vertical fractures of the White Limestone and the NNE striking fault from which MKR waters discharge probably facilitates upward flow of deep circulating waters (Hylton, 1987).

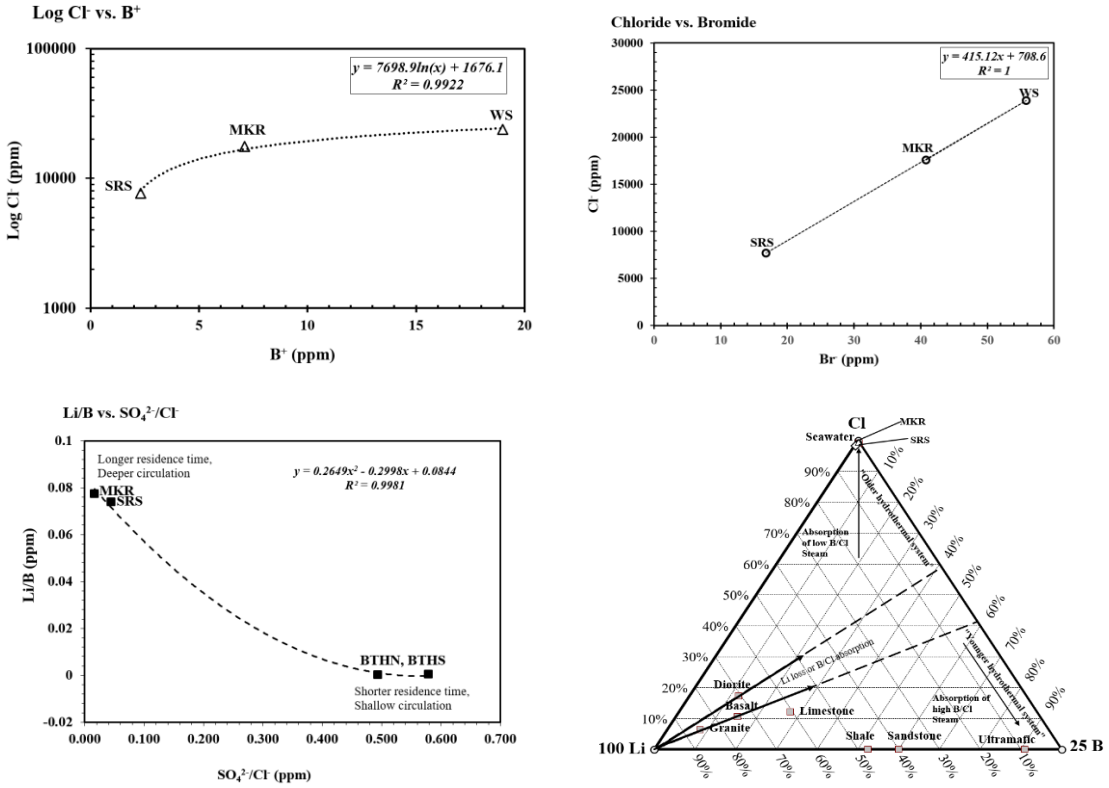

Figure 5: a. Log Cl/B plot for three springs with the highest total dissolved solids (TDS) concentration on the island of Jamaica: MKR, SRS, and WS, b. Linear plot of Chloride (Cl^-) vs. bromide (B^+), c. Cl/SO_4 vs. Li/B ratios used to classify MKR waters based on depth. Cl^- increases with depth with regard to SO_4^2, d. Cl-Li-B ternary diagram (Giggenbach, 1991) plot of the Milk River (MKR) and SRS water samples.

4.1.2 Stable Isotope Analysis

Stable isotopic (i.e. $\delta^{18}O$ and δ^2H) analyses may be used to provide information on the origin, age, steam separation, extent of water-rock interaction of the discharged fluids, and mixing between deep and shallow waters from different sources from water samples (Kharaka and Thordsen, 1992). The isotopic composition for MKR and SRS waters ($\delta^{18}O$ = 0.61‰; δ^2H = 2.70‰) and (-2.46‰; -14.70‰) were compared to the Global Meteoritic Water Line (Craig, 1961) (Figure 6). MKR water plots in the "seawater" field to the right of the GMWL where it has a $\delta^{18}O$ shift (enrichment). SRS water plots very close to the right of the GMWL, but is depleted in $\delta^{18}O$ and δ^2H. The MKR $\delta^{18}O$ enrichment confirms extensive water-rock interaction and evaporation of the brine (Figure 6). MKR possibly represents a mixture of closer to ≈ 95% saltwater and 5% fresh water. The MKR isotope signature show the water has evolved through deep circulation and mixing of saline geothermal fluids with very minimal or no recharge (Figure 6). Ion data, ionic ratios, and isotope signatures confirm MKR water is the original seawater-derived brine source from which the SRS brine is derived prior to shallow mixing with cold, freshwater. The isotopic signature of the SRS brine indicates some mixing with cold meteoritic recharge or groundwater at very shallow depths. Differences in temperature and δ^2H and $\delta^{18}O$ signatures distinguish MKR as a Na-Cl geothermal brine from SRS which is a cold Na-Cl brine. During the ascent of geothermal water from a reservoir to the surface, it travels through interconnected fractures where it discharges as hot springs, may cool by conduction, mix with meteoritic or colder water, undergo boiling, or be impacted by a combination of these processes.

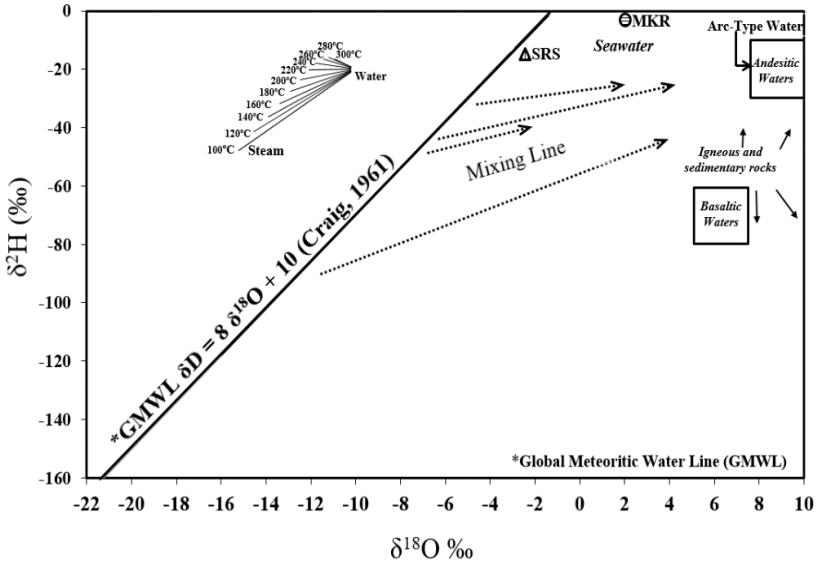

Figure 6: Variation in $\delta^{18}O$ and $\delta^{2}H$ for the MKR and SRS waters. GMWL = Global Meteoritic Water Line ($\delta^{2}H = \delta^{18}O + 10$; After Craig 1961).

4.2 Geothermometry

The MKR discharge temperature (36.9°C) was modeled geothermometric equations using SOLGEO and Rockware AqUA®. Table 2 lists a range of temperatures (87°C – 206°C) estimated for the depth to circulation and MKR geothermal reservoir from silica (SiO_2) and cation (Na/K, Na-K-Ca, Na-K-Mg) geothermometers. The Na-K-Mg ternary geoindicator (Giggenbach, 1988) is used to distinguish the equilibrium status in geothermal systems and the level of mixing by the inter-relations among Na, K, and Mg (Figure 7) in geothermal fluids. The Na-K-Ca (Fournier and Truesdell, 1973) geothermometer was used to eliminate the possible effect of Ca on the Na-K geothermometer.

Table 2: Temperature equations (in °C) for silica and cation geothermometers

Geothermo-meter	Equation	Estimate MKR (°C)	Range (°C)	Source
SiO_2	$42.198 + 0.28831S - 3.6686\,x\,10^{-4}S^2 + 3.1665\,x\,10^{-7}S^3 + 77.034 LogS$	81	NR	Fournier and Potter (1982)
Na-K	$T_{Na/K} = \left[\frac{1535}{0.989 - log\,S}\right] - 273.15$	153	100-275	Truesdell (1977)
Na-K	$T_{Na-K} = \frac{876.3(\pm 26.26)}{log\left(\frac{Na}{K}\right) + 0.8775(\pm 0.0508)} - 273.15$	159	30-350	Santoyo & Diaz-Gonzalez (2010)
Na-K	$T_{Na-K} = \frac{833}{(0.78 + log\left(\frac{Na}{K}\right)} - 273.15$	161	NR	Tonani (1980)
Na-K	$T_{Na/K} = \left[\frac{1319}{log\left(\frac{Na}{K}\right) + 1.699}\right] - 273.15$	162	25-350	Arnórsson et al. (1) (1983b)
Na-K	$T_{Na/K} = 733.6 - 770.551[\log\left(\frac{Na_m}{K_m}\right) + 378.189[log\left(\frac{Na_m}{K_m}\right)^2 - 95.753[log\left(\frac{Na_m}{K_m}\right)^3\ 9.5444[log\left(\frac{Na_m}{K_m}\right)^2$	173	0-350	Arnórsson et al. (2) (2000)
Na-K	$T_{Na/K} = \left[\frac{1178}{log\left(\frac{Na}{K}\right) + 1.239}\right] - 273.15$	177	NR	Nieva & Nieva (1987)
Na-K	$T_{Na/K} = \left[\frac{1052}{1 + e\left(1.714\,log\left(\frac{Na}{K}\right) + 0.252\right) + 76}\right]$	179	100-350	Can (2002)
Na-K	$T_{Na/K} = \left[\frac{1289(\pm 76}{log\left(\frac{Na}{K}\right) + 0.615}\right] - 273.15$	193	NR	Verma & Santoyo (1997)
Na-K	$T_{Na/K} = \left[\frac{1217(\pm 93.9)}{log\left(\frac{Na}{K}\right) + 1.483}\right] - 273.15$	195	0-250	Fournier (1979)
Na-K-Mg	Na-K-Mg Ternary Diagram	206	60-340	Giggenbach (1988)
Na-K-Ca	$T_{Na-K-Ca} = \left[\frac{1647}{log\left(\frac{Na_m}{K_m}\right) + \beta\left(Log\left(\frac{Ca^{0.5}{}_m}{Na_m}\right) + 2.06\right) + 2.47}\right] - 273.15$	206	0-250	Fournier & Truesdell (1973)
Na-K/Mg-Ca*	$10cMg/(10cMg + cCa)$ vs. $10cK/(10cK + cNa)$	130	40-340	Giggenbach (1988)

Overall, reservoir temperatures estimated from silica geothermometers (87-89°C) for MKR were lower than estimated temperatures from cation geothermometers (153-206°C). Lower temperature estimates from silica geothermometers may be due to precipitation of silica during ascent of the waters or dilution by waters of comparatively lower silica content. MKR plots in the 'partially equilibrated' and 'seawater' fields of the Giggenbach (1988) geoindicator and the reservoir temperature was estimated to be 200°C

(Figure 7). Geothermal water chemistry is characterized by equilibrium states that exist between solutes and alteration minerals at relatively high temperatures whereas the chemistry of cold water is determined by the kinetics of the leaching process (Arnórsson, 1985). SRS plots in the 'immature waters' field and close to seawater. Fluids may undergo 'partial' or 'full equilibration' during interaction with the mineral-rock surface of fractures undergo temperature decrease during ascent. Hence the application of various geothermometers to the same field frequently yield different values for reservoir temperature. SRS is expected to plot in the immature field because it underwent mixing with cold groundwater. The observation that neither MKR nor SRS have attained chemical equilibrium in the fluid may be explained re-equilibration, mixing, and dilution during the ascent of the geothermal brine. The geotemperature estimated for MKR using the Na-K-Mg Giggenbach (1988) geoindicator (Figure 6) was higher slightly higher than temperature estimates from Na-K geothermometers (153-197°C), but 6°C lower than the geotemperature (206°C) yielded the Na-K-Ca geothermometers. Verma et al. 2008 discourages the use of K-Mg, Na-Li, Na-K-Ca, Na-K-Mg, and Na-K-Ca-Mg geothermometers that have led to errors, but deem the Na-K geothermometers more appropriate for providing more reliable results. Na^+ and K^+ take longer to re-equilibrate based on feldspar content, the Na-K geothermometer may be more appropriate to estimate temperatures areas of deep circulation and longer residence time. Cation geothermometers (e.g. Na/K) are useful where mixing is suspected, because they are less affected by dilution or steam loss given that they are based on ion ratios and re-equilibration is slower compared to the silica quartz geothermometer. If re-equilibration or dilution from shallow mixing with other fluids occurs during ascent along the flow path, only the minimum estimate of the highest temperature reached in the geothermal reservoir would have be detected (Grasby and Hutcheon, 2001).

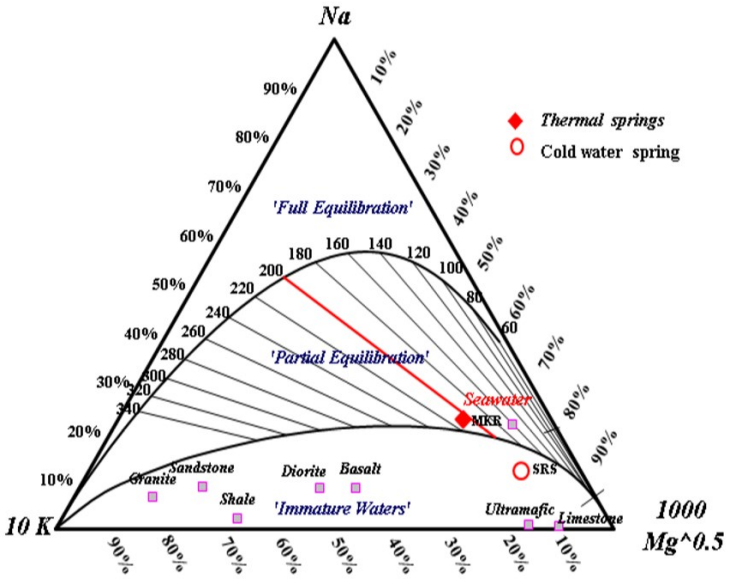

Figure 7: Comparison of graphical evaluation of water-rock interaction equilibration temperatures for MKR and SRS waters using Na-K-Mg concentrations (in mg/kg) (Giggenbach, 1988).

4.2.1 Conceptual Model of the Milk River Geothermal System

The minimum depth to the geothermal MKR source was determined using an average geothermal gradient of 30°C/km for the Caribbean region at (i.e. 153°C/30°C/km) = 5.10 km). The variation in the Na-Cl mass ratios for MKR and SRS may be attributable to the depth of circulation and fluid migration controlled by the SCFZ fracture network. The hydrochemistry confirms a Na-Cl type, radioactive water that undergoes extensive water-rock interaction with evaporate-based rocks and becomes heated during its long ascension through the along fractures to the SCFZ at high flow velocities. MKR and SRS waters originate from a common source of deep circulating Na-Cl type brine that is heated as it migrates through long pathways in fractures, inducing non-volcanogenic geothermal conditions at depth. The flow of geothermal brine is expected to migrate under the hydrotectonic control of fractures associated with South Coast fault Zone (SCFZ) both parallel and transverse to it, or may act as a barrier to flow in some areas along the fault zone. The occurrence of radioactivity and other hydrochemical characteristics of Milk River thermal spring (MKR) and Salt River cold water spring (SRS) are likely to be related to hydrotectonic control of the E-W striking SCF and its associated fractures. The regional tectonic setting of the SCF and its close proximity to the MKR and SRS sites, including vertical fractures of the White Limestone and the NNE striking fault from which the MKR water discharges. It may be inferred that the permeability of the fault and fracture network facilitates high velocity upward flow of deep circulating waters, hence the dominance of the chloride concertation in the water. The hydrochemical processes that contributed to the evolution and depth of circulation of MKR and SRS waters have been determined from analyses of the hydrogeochemistry, pattern recognition, δ^2H and $\delta^{18}O$ isotope analyses, and estimated reservoir temperatures. By coupling these results with the geological and tectonic settings, it was possible to a draw a simplified conceptual model (Figure 8) to hypothesize the hydrodynamics attributed to the evolution and composition of MRK and SRS waters.

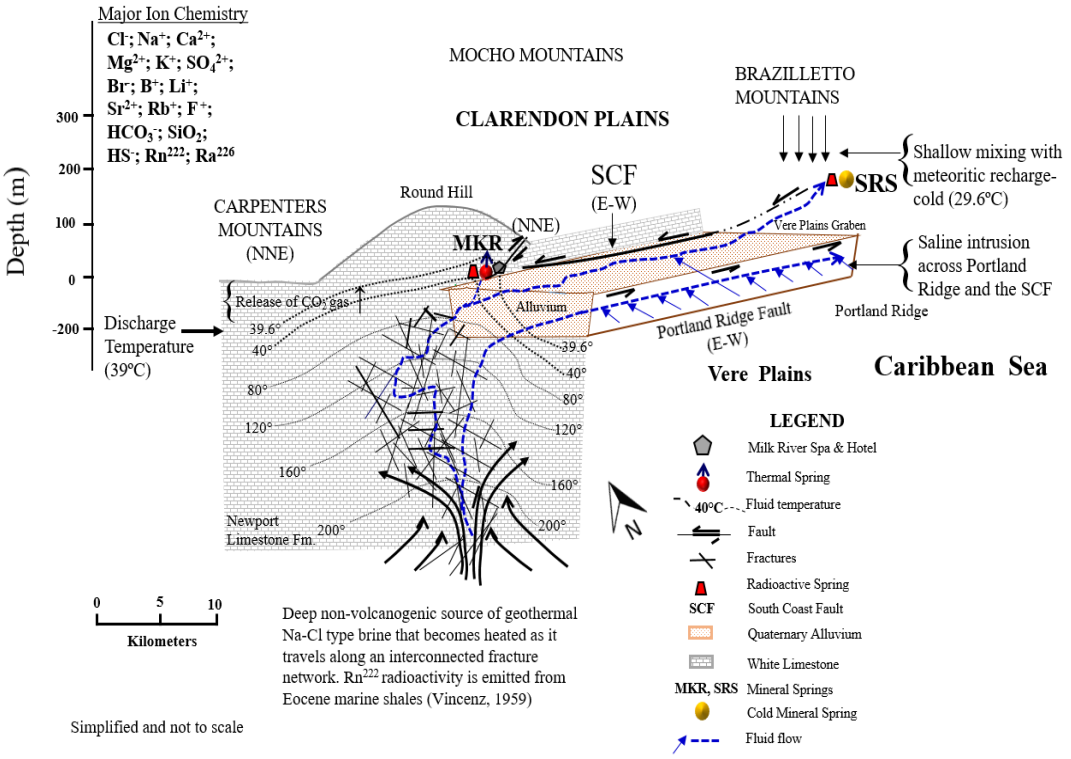

Figure 8: Conceptual model of the chemical processes and hydrodynamics of a MKR and SRS showing the circulation of fluids, based on hydrochemistry, pattern recognition, geothermometry and their close proximity to the South Coast Fault (SCF).

5. CONCLUSION

MKR and SRS waters are classified as Na-Cl type waters. The variation in the Na-Cl mass ratios for MKR and SRS may be attributable to the depth of circulation and fluid migration controlled by the SCFZ fracture network. Na-Cl waters are typical of marine and deep ancient ground waters. It is inferred from the hydrochemistry, a Na-Cl type, radioactive water undergoes extensive water-rock interaction with evaporate-based rocks and becomes heated during its long ascension through the along fractures to the SCFZ at high flow velocities. Ion data and ionic ratios confirm MKR water is the original seawater-derived brine source from which the SRS brine is derived prior to shallow mixing with cold, freshwater. In essence, MKR and SRS waters appear to originate from one common source of deep circulating Na-Cl type brine that is heated as it migrates through long pathways in fractures and induces non-volcanogenic geothermal conditions at depth. Isotope signatures corroborate the MKR water as the original seawater-derived brine source from which the SRS brine is derived prior to shallow mixing with cold, freshwater. The thermal character of the MKR water and the δ^2H- $\delta^{18}O$ isotope signatures distinguish it as a geothermal brine (>10000 mg/L Cl^-) from SRS which is a cold Na-Cl brine. During the ascent of geothermal water from a reservoir to the surface, it travels through interconnected fractures where it discharges as hot springs at MKR, travels along fractures to east and mixes with meteoritic/colder groundwater or a combination of these processes before discharging at SRS. Ion ratios of Li/B vs. SO_4/Cl indicate deep circulating fluid signatures of MKR and SRS derived mainly from extensive water/rock interactions involving mainly clastic rocks. The presence of strontium (Sr^{2+}) appears to be related to water-rock interaction with the volcanic basement and fluid-fluid mixing in the MKR and SRS samples. The occurrence, radioactivity and other similar hydrochemical characteristics of Milk River thermal spring (MKR) and Salt River cold water spring (SRS) are likely to be related to hydrotectonic control of the E-W striking SCF and its associated fractures.

MKR represents a low temperature/low enthalpy (156°- 250°C) geothermal resource with an average reservoir temperature estimated at about 176°C. Based on the very minor limitations, geotemperatures estimated from Na-K geothermometers were deemed more reliable than geotemperatures yielded by silica geothermometers. The regional tectonic setting of the SCF and its close proximity to the MKR and SRS sites, including vertical fractures of the White Limestone and the NNE striking fault from which the MKR water discharges facilitate the high velocity upward flow of deep circulating waters. The hydrochemical processes that contributed to the evolution and depth of circulation of MKR and SRS waters have been determined from analyses of the hydrogeochemistry, pattern recognition, δ^2H and $\delta^{18}O$ isotope analyses, and estimated reservoir temperatures. By coupling these results with the geological and tectonic settings, it was possible to a draw a simplified conceptual model to hypothesize the hydrodynamics attributed to the evolution and composition of MRK and SRS waters. In conclusion, the results of this work demonstrate the integration of hydrogeochemical analysis and modeling, pattern recognition, geothermometry, and information on the geological and tectonic setting is a very useful approach to preliminary characterization of geothermal resources prior to exploratory drilling and development.

ACKNOWLEDGEMENTS

This investigation was partially funded by National Science Foundation (NSF) ADVANCE LEADER minigrants Grants No. 8449 and No. 8451 from Wright State University and Central State University, Ohio.

REFERENCES

Arden, D. D.: Geology of Jamaica and the Nicaragua Rise. In: Nairn A.E.M., Stehli F.G. (Eds.), The Gulf of Mexico and the Caribbean, (1975), Springer, Boston, MA.

Arnórsson, S., Gunnlaugsson, E., and Svavarsson, H.: The Chemistry of Geothermal Waters in Iceland III: Chemical Geothermometry in Geothermal Investigations, *Geochimica et Cosmochimica Acta*, **47**, (1983). 567-577.

Arnórsson, S.: The use of Mixing Models and Chemical Geothermometers for Estimating Underground Temperatures in Geothermal Systems, *Journal of Volcanology and Geothermal Research*, **23**(3-4), (1985), 299-335.

Arnórsson, S.: The Quartz and Na/K Geothermometers: I. New Thermodynamic Calibration, in Proceedings World Geothermal Congress, (2000), Kyushu Tohoku, Japan, 929-934.

Barnett, W. L.: Some Chemical Analyses of the Water from Mineral Springs in Jamaica, Handbook of Jamaica 1947-1948, Kingston, (1923), pp 536-539.

Benford, B., DeMets, C., and Calais, E.: GPS Estimates of Microplate Motions, Northern Caribbean: Evidence for a Hispaniola Microplate and Implications for Earthquake Hazard, *Geophysical Journal International*, **191**, (2012b), 481–490.

Benford, B., Tikoff, B., and DeMets, C.: Interaction of Reactivated Faults within a Restraining Bend: Neotectonic Deformation of Southwest Jamaica, *Lithosphere*, **7**(1), (2015), 21-39.

Brondi, M., Dall'Aglio, M., and Vitrani, F.: Lithium as a Path Finder Element in Large Scale hydrogeochemical exploration for hydroheothermal systems, *Geothermics*, **2**(3-4), (1973), 142-153.

Brondi, M., Fidelibus, M. D., Gragnan, I. R., and Tulipano, L.: Hydrochemical Study of and Distribution of Some Trace Elements in the Most Important Coastal Springs and Groundwater of the Apulian Region (Southern Italy), *Geologia Applicatta et Idrolgeologia*, XVII, (1983), 65-80.

Caine, J. S., Evans, J. P., and Forster, C. B.: Fault Zone Architecture and Permeability Structure, *Geology*, **24**, 1025-1028.

Can, I.: A New Improved Na/K Geothermometer by Artificial Neural Networks, *Geothermics*, **31**(6), (2002), 751-760.

Chebotarev, I. I.: Metamorphism of Natural Water in the Crust of Weathering I, II, & II, *Geochimica et Cosmochimica Acta,* **8**, (1955), 22-212.

Collins, A. G.: Geochemistry of Oilfield Brines, Elsevier, Amsterdam, (1975), 496 pp.

Craig, H.: Isotopic Variations in Meteoric Waters, *Science* **133**, (1961), 1702-1703.

Cruz, J. V., and Franca, Z.: Hydrogeochemistry of Thermal and Mineral Water Springs of the Azores Archipelago (Portugal), *Journal Volcanology and Geothermal Research*, **151**, (2006). 382-398.

Dassi, L.: Investigation by Multivariate Analysis of Groundwater Composition in Multilayer Aquifer System from North Africa: A Multi-Tracer Approach. *Applied Geochemistry,* **26**, (2011), 1386-1398.

Delgado-Outeiriño, I., Araujo-Nespereira, P., Cid-Fernández, P., Mejuto, J. A., Martínez-Carballo, J. C., and Simal-Gándara, J.: Behaviour of Thermal Waters Through Granite Rocks Based on Residence Time and Inorganic Pattern, *Journal of Hydrology*, **373**, (2009), 329-336.

Dominguez L., Andreani, L., Stanek, K. P., and Gloaguen, R.: Geomorpho-Tectonic Evolution of the Jamaican Restraining Bend, *Geomorphology*, **228**, (2015), 320-334.

Draper, G.: Geologic and Tectonic evolution of Jamaica. University of the West Indies Mona, *Contributions to Geology*, **3**, (1988), 3-9.

Drever, J., Holland, H., and Turekian, K.: (Eds.) Surface and Groundwater, weathering, and soils (Vol. Treatise on Geochemistry. Oxford: Elsevier Ltd, (2004).

Durov, S. A.: Natural Waters and Graphic Representation of their Composition, *Doklady Akademii Nauk SSSR*, 59, (1948), 87-90.

Fontes, J.C., and Matray, J. M.: Geochemistry and Origin of Formation Brines from the Paris Basin, France, *Chemical Geology*, **109**, (1993), 177-200.

Fournier, R. O., and Truesdell, A. H.: An Empirical Na-K-Ca Geothermometer for Natural Waters, *Geochimica et Cosmochimica Acta*, **37**(5), (1973), 1255-1275.

Fournier, R. O.: Chemical Geothermometers and Mixing Models for Geothermal Systems, *Geothermics*, **5**, (1977), 41-50.

Fournier, R.O., and Potter, R. W.: A Revised and Expanded Silica (quartz) Geothermometer, *Geothermal Resources Council Bulletin* **11**, (1982). 3-12.

Giggenbach, W. F.: Geothermal Solute Equilibria. Derivation of Na-K-Mg-Ca Geoindicators. *Geochimica et Cosmochimica Acta*, **52**, (1988). 2749-2765.

Giggenbach, W.F. and Goguel, R.L.: Collection and Analysis of Geothermal and Volcanic Water and Gas Discharges, DSIR report CD 2401, 4th Ed., (1989), Pentone, New Zealand.

Giggenbach, W. F.: Chemical Techniques in Geothermal Exploration. In: Application of in Geothermal Reservoir Development, D'Amore, F. (Ed.), Rome, (1991), pp. 252-270.

Grasby, S. E., and Hutcheon, I.: Controls on the Distribution of Thermal Springs in Southern Alberta and British Columbia, *Canadian Journal of Earth Sciences*, **38**, (2001), 427-440.

Howard K. W. F., and Mullings, E.: Hydrochemical Analysis of Groundwater Flow and Saline Incursion in the Clarendon Basin, Jamaica, *Groundwater*, **34**(5), (1996), 801-810.

Hylton, H. A.: The Mineral Springs of Jamaica, *Geological Survey Division, Bulletin* **11**, (1987), Ministry of Mining, Energy and Tourism, Jamaica, 1-69.

Kharaka, Y. K., and Thorsden, J. J.: Stable Isotope Geochemistry and the Origin of Water in Sedimentary Basins. In Isotope Signatures and Sedimentary Records (Eds. N. Clauer and S. Chaudhuri). Springer, Berlin, (1992), 411-466.

Kharaka, Y. K., and Hanor, J.: Deep fluids in the continents: Sedimentary Basins, In J. Drever, H. Holland, & K Turekian (Eds.), Surface and Groundwater, Weathering and Soils (Vol. Treatise on Geochemistry), (2004), pp 499-540.

Knauth, P. L.: Origin and Mixing History of Brines, Palo Duro Basin, Texas, U. S. A., *Applied Geochemistry*, **3**, (1988), 455-474.

Lemarchand, D., Gaillardet, J., Lewin, È., and Allègre, C. J.: Boron Isotope Systematics in Large Rivers: Implications for the Marine Boron Budget and Paleo-pH Reconstruction over the Cenozoic, *Chemical Geology*, **190**, (2002), 123–140.

Lee, K., Kim, T., Byrne, R. H., Millero, F. J., Feely, R. A., and Liu, Y.: The Universal Ratio of Boron to Chlorinity for the North Pacific and North Atlantic Oceans, *Geochimica et Cosmochimica Acta*, **74**, (2010), 1801–1811.

Leeman Sisson, V. P.: Geochemistry of Boron and its Implications for Crustal and Mantle Processes, *Reviews in Mineralogy*, **33**, 845-707.

Lewis, J.F., and Draper, G.: Geology and tectonic evolution of the Northern Caribbean Margin. In: Dengo, G., Case, J. E. (Eds.), The Caribbean Region (The Geology of North America, Vol. H). Geological Society of America, Boulder, CO, (1990), pp. 77–140.

Lopez-Chicano, M. J., Céron, C., Vallejos, A., and Pulido-Bosch, A.: Geothermal Chemistry of Thermal Springs, Alhama de Granada (southern Spain), *Applied Geochemistry*, **16**, (2001), 153-1163.

Mann, P., DeMets, C., and Wiggins-Grandison, M.: Towards a Better Understanding of the Late Neogene Strike-Slip Restraining Bend in Jamaica: Geodetic, Geological, and Seismic Constraints, In W.D. Cunningham, W. D. and Mann, P. (Eds.), Tectonics of Strike-Slip Restraining and Releasing Bends. Geological Society of London Special Publication 290, (2007), p. 239-253, doi:10 10.1144/SP290.8.

Meschede, M., and Frisch, W.: A Plate-Tectonic Model for the Mesozoic and Early Cenozoic History of the Caribbean plate. *Tectonophysics,* **296**, (1998), 269-291.

Mohammadi, Z., Bagheri, R., and Jahanshahi, R.: Hydrogeochemistry and Geothermometry of Changal Thermal Springs, Zagros Region, Iran, *Geothermics*, **39**, (2010), 242-249.

Nieva, D., and Nieva, R.: Developments in Geothermal Energy in Mexico-Part Twelve: A Cationic Geothermometer for Prospecting of Geothermal Resources, *Heat Recovery Systems*, **7**(3), (1987), 243-258.

Pasvanoğlu, S.: Hydrogeochemistry of Thermal and Mineralized Waters in the Diyadin (Ağri) Area, Eastern Turkey, *Applied Geochemistry*, **38**, (2013), 70-81.

Piper, A. M.: A Graphical Procedure in the Geochemical Interpretation of Water Analysis. Eos, Transactions of American Geophysical Union, **25**(6), 914-928.

Robinson, E.: In: Donovan S. K., Jackson TA (Eds.). Jamaica. In Caribbean Geology: An Introduction, University of the West Indies Publishers' Association, Kingston, (1994), pp. 111-127.

Roobol, M. J.: Post-Eruptive Mechanical Sorting of Pyroclastic Material and Example from Jamaica, *Geological Magazine*, **113**, (1976), 429-440.

Sanchez-Martos, F., Pulido Bosch, A., Vallejos, A., Molina, L., J., and Gisbert, J.: Rasgos Hidogeoquímicos de las Aguas Termales en los Aquíferous Carbonatados del Bajo Andrax (Almeria), *Geogaceta*, **35**, (2004), 171-174.

Santoyo, E., and Díaz-Gonzaleź, L.: A New Improved Proposal of the Na/K Geothermometer to Estimates Deep Equilibrium Temperatures and Their Uncertainties in Geothermal Systems, *Proceedings*, the World Geothermal Congress, April 25-29, 2010, Bali, Indonesia.

Schoeller, H.: Leseaux Souterraines, Mason and Cie. Paris, (1962), 642p.

Shakeri, A., Moore, F., and Kompani-Zare, M.: Geochemistry of the Thermal Springs of Mount Taftan, southeastern Iran, *Journal of Volcanology and Geothermal,* Research, **178**, (2008), 829-836.

Taylor, S. A. G., and Chubb, L. J.: Hydrogeology of the Clarendon Plains, Proceedings of the Geologists' Association **68**(3), (1957), 204-210.

Tonani F.: Some Remarks on the Application of Geochemical Techniques in Geothermal Exploration. In: Proceedings of the Advances in European Geothermal Resources, Second Symposium, (1980), Strasbourg, pp. 428–443.

Truesdell A. H., and Fournier R.O.: Procedure for Estimating the Temperature of a Hot Water Component in a Mixed Water by Using a Plot of Dissolved Silica Versus Enthalpy, *Journal of Research of the U. S. Geological Survey*, **5**, (1977), 49-52.

Uhlman, K.: The Geochemistry of Boron in a Landfill Monitoring Program, *Groundwater Monitoring Review*, **11**, (1991), 139-143.

Verma, M.P., and Santoyo E.: New Improved Equations for Na/K, Na/Li and SiO_2 Geothermometers by Outlier Detection and Rejection, *Journal of Volcanology and Geothermal Research*, **79**(1-2), (1997), 9-24.

Verma, S. P., Pandarinath, K., Santoyo, E.: SolGeo: A New Computer Program for Solute Geothermometers and its Application to Mexican Geothermal Fields, *Geothermics*, **37**, (2008), 597-621.

Vincenz, S. A.: Some Observations of Gamma Radiation Emitted by a Mineral Spring in Jamaica, *Geophysics*, **7**(4), (1959), 422-434.

Wadge, G. S., Brookes, S., and Royall, M.: Structure Models of the Lower Vere Plains, Jamaica, *Journal of the Geological Society of Jamaica,* **22**, (1982), 1-6.

Zans, V. A.: Bath Springs, St. Thomas: Their History and Development, *Journal of the Geological Society of Jamaica*, **4**, (1961), 47 -67.